

Analytic determination of dynamical and mosaic length scales in a Kac glass model

S. Franz^{1,3} and A. Montanari^{2,3}

¹ *The Abdus Salam ICTP, Strada Costiera 11, P.O. Box 586, I-34100 Trieste, Italy*

² *Laboratoire de Physique Théorique de l'Ecole Normale Supérieure, CNRS-UMR 8549 and*

³ *Isaac Newton Institute for Mathematical Sciences 20 Clarkson Road, Cambridge, CB3 0EH, U.K.*

(Dated: December 2, 2024)

We consider a disordered spin model with multi-spin interactions undergoing a glass transition. We introduce a dynamic and a static length scales and compute them in the Kac limit (long-but-finite range interactions). They diverge at the dynamic and static phase transition with exponents (respectively) $-1/4$ and -1 . The two length scales are approximately equal well above the mode coupling transition. Their discrepancy increases rapidly as this transition is approached. We argue that this signals a crossover from mode coupling to activated dynamics.

PACS numbers: 05.20.-y (Classical statistical mechanics), 64.70.Pf (Glass transitions), 75.10Nr (Spin-glass and other random models)

The relaxation mechanisms of supercooled liquids near the glass transition are today poorly understood. For moderate supercooling, mode coupling theory (MCT) captures several important dynamical features, such as time scale separation and the relation between α and β relaxation [1]. Unfortunately MCT fails at low temperature since it predicts a spurious power law divergence of the relaxation time at an ergodicity breaking temperature T_d .

A partial elucidation of ergodicity restoration below T_d originated from the remark that MCT is exact for some mean-field disordered spin models [2]. In this context, the relaxation time divergence at T_d finds its root in the proliferation of metastable states with diverging lifetime. The existence of such states provides the basic ergodicity restoration force in finite dimension. Phenomenological droplet arguments based on this mean field picture [3, 4] predict in fact the existence of about $\exp\{\Sigma\ell^d\}$ different states at length scale ℓ , while a given boundary condition can select one of them by raising the free energy of the others by at most $\Delta F = \sigma\ell^\theta$ with $\theta \leq d - 1$. Balancing these two forces yields a “mosaic length” $\ell_s \approx (\beta\sigma/\Sigma)^{\frac{1}{d-\theta}}$, above which the system is thermodynamically a liquid.

The above picture suggests that the typical size of ergodicity restoring rearrangements is determined by thermodynamics. According to an alternative intuition (largely inspired by kinetically constrained models [5]), as the temperature is lowered, it becomes impossible to relax local degrees of freedom through purely local moves. The relevant length scale is essentially dynamical and corresponds to the size of cooperative rearrangements.

In both scenarios, the typical size of rearranging regions can be characterized by a dynamical (four points) susceptibility and a corresponding dynamical length ξ_d [6, 7]. Recent experiments on colloidal systems and supercooled liquids have indeed revealed a marked increase of ξ_d close to the glass transition [8]. Within MCT, ξ_d has been shown to diverge at T_d [6, 7] with no static

counterpart.

A relation between mosaic length and the dynamical length ξ_d was first noticed by Jack and Garrahan [9] in a plaquette glass model. However a detailed theoretical description of this relation is lacking.

The aim of this letter is to present the first analytic calculation of the mosaic length scale, and its comparison with the dynamical length computed in a unified framework. To this end we study a disordered model with Kac interactions [10, 11] and define length scales through properly chosen point-to-set correlation functions. We are thus able to answer some fundamental open questions, such as their relative order of magnitude in different temperature regimes.

It is well known that conventional static correlation functions do not show any signature of a large length scale in supercooled liquids. In order to circumvent this problem, we define length scales through “point-to-set” correlations [4, 12]. We fix a reference configuration $\underline{s}^{(\alpha)} = \{s_x^{(\alpha)}\}_{x \in \mathbb{Z}^d}$ drawn from the equilibrium Boltzmann measure, and consider a second configuration \underline{s} that is constrained to be close to $\underline{s}^{(\alpha)}$ outside a sphere $B_{x_0}(\ell)$ of radius ℓ centered at a particular point x_0 . In introducing the static correlation length ℓ_s , \underline{s} is distributed according to the Boltzmann law inside $B_{x_0}(\ell)$ with a boundary condition determined by $\underline{s}^{(\alpha)}$. We then define ℓ_s to be the smallest value of ℓ such that the correlation between $\underline{s}^{(\alpha)}$ and \underline{s} at the center of $B_{x_0}(\ell)$ (as measured through a correlation function, e.g. $\langle s_{x_0}^{(\alpha)} s_{x_0} \rangle_{\text{conn}}$) decays below a preassigned value ε .

Consider now a particular choice of local stochastic dynamics verifying detailed balance. Let τ be the auto-correlation time for a local degree of freedom. As shown in Ref. [13], in a finite range system, one has necessarily $C_1 \ell_s \leq \tau \leq \exp(C_2 \ell_s^d)$, with C_1 and C_2 two model dependent constants. The lower bound corresponds to a MCT-like dynamics, a good description for $T \gg T_d$ (up to a non-trivial scaling exponent, i.e. $\tau \sim \ell_s^z$ with $z \geq 1$). The upper bound corresponds instead to the ac-

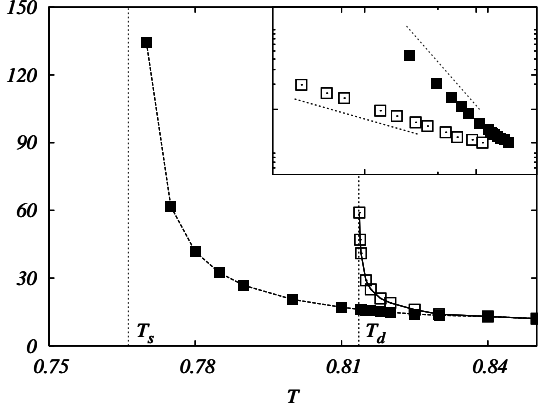


FIG. 1: Dynamic (empty squares) and static (filled squares) rescaled lengths $\hat{\ell}_d$ and $\hat{\ell}_s$, for a Kac model with two and four spin interactions. The vertical lines correspond to the mode coupling and thermodynamic glass transitions $T_d \approx 0.813526$ and $T_s \approx 0.766287$. In the inset, the rescaled lengths as functions of $(T - T_d)$ (for $\hat{\ell}_d$) and $(T - T_s)$ (for $\hat{\ell}_s$). The dotted lines have slope (respectively) $-1/4$ and -1 .

tivated behavior that should hold below T_d (we expect $\tau \sim \exp(\ell_s^\psi)$ with $\psi \leq d - 1$). In a model with large-but-finite interaction range γ^{-1} (see below), one finds $\ell_s(T, \gamma) \approx \gamma^{-1} \hat{\ell}_s(T)$, and the two types of dynamics can be distinguished sharply (exponentially in $1/\gamma$).

The two regimes can be bridged defining a new dynamical length ℓ_d which separates scales $\ell \gg \ell_d$ on which non-activated relaxation is possible, from scales $\ell \ll \ell_d$ on which activation is necessary. In order to precise this notion, consider a system initialized by setting $\underline{s}(t=0) = \underline{s}^{(\alpha)}$ and constrained to remain close to $\underline{s}^{(\alpha)}$ outside $B_{x_0}(\ell)$ at all subsequent times, and let $\tau(\ell)$ be the shortest time such that $\langle s_{x_0}(0) s_{x_0}(t) \rangle_{\text{conn}}$ decays below ε . By the above definition $\tau(\ell) = \infty$ for $\ell < \ell_s$. We define ℓ_d by the property that $\tau(\ell)$ is (exponentially) divergent as $\gamma \rightarrow 0$ for $\ell < \ell_d$, and stays bounded for $\ell > \ell_d$.

In the following we shall compute ℓ_s and ℓ_d in a d -dimensional spherical p -spin disordered model with Kac interactions. Its elementary degrees of freedom are soft spins $s_i \in \mathbb{R}$, associated to the vertices of a cubic lattice of size $2L$ (i.e. $i \in \{-L+1, \dots, L\}^d$), with periodic boundary conditions. Given the interaction range $\gamma^{-1} > 0$ and a non-negative rapidly decreasing function $\psi : \mathbb{R}_+ \rightarrow \mathbb{R}_+$, normalized by $\int \psi(|x|) d^d x = 1$, we define the local overlap of two configurations $\underline{s}^{(1)}$ and $\underline{s}^{(2)}$ as $Q_{12}(i) = \gamma^d \sum_j \psi(\gamma|i - j|) s_j^{(1)} s_j^{(2)}$. The local spherical constraint is $Q_{11}(i) = \gamma^d \sum_j \psi(\gamma|i - j|) s_j^{(1)} s_j^{(1)} = 1$. The Hamiltonian $H(\underline{s})$ is a quenched Gaussian random variable of zero mean and covariance $\mathbb{E}[H(\underline{s}^{(1)}) H(\underline{s}^{(2)})] = \sum_i f(Q_{12}(i))$ where $f(x)$ is a polynomial with positive coefficients. In the following we shall use as running example the polynomial $f(x) = \frac{1}{10} x^2 + x^4$ (i.e. a model with two and four spin interactions) in $d = 2$ dimensions (but the critical

behavior is independent of $d \geq 2$). While the quartic term in the polynomial assures the wanted phenomenology at the mean-field level, the relatively small quadratic term is introduced to have a regular gradient expansion of the free-energy functional (see below and [11]). The Kac limit is defined as $L \gg \gamma^{-1} \gg 1$ (in other words, the limit $\gamma \rightarrow 0$ is taken *after* $L \rightarrow \infty$). It is convenient to define the rescaled lengths $\hat{\ell}_{s/d} \equiv \gamma \ell_{s/d}$ that admit a finite limit as $\gamma \rightarrow 0$. In Fig. 1 we plot $\hat{\ell}_d$ and $\hat{\ell}_s$ as functions of temperature for our running example, in the Kac limit. They diverge at two distinct temperatures $T_d \approx 0.813526$ and $T_s \approx 0.766287$. The dynamical length diverges as $\hat{\ell}_d \sim (T - T_d)^{-1/4}$. This is the same behavior as (independently) found within MCT for the length ξ_d [6, 14], we therefore identify ℓ_d with ξ_d . The static length behaves as $\hat{\ell}_s \sim 1/\Sigma(T) \sim (T - T_s)^{-1}$ corresponding to $\theta = d - 1$.

We shall now explain how the lengths ℓ_d and ℓ_s have been computed. Consider a reference configuration $\underline{s}^{(\alpha)}$, a sphere $B_0(\ell)$ with radius ℓ , centered at $x = 0$, and let $\bar{q} \leq 1$. We introduce the constrained Boltzmann measure $\langle \cdot \rangle_\ell^\alpha$ by setting

$$\langle \mathcal{O} \rangle_\alpha^\ell = \frac{1}{Z_\alpha} \int_{\underline{s}} \mathcal{O}(\underline{s}) e^{-\beta H(\underline{s})} \prod_{i \notin B_0(\ell)} \delta(Q_{\underline{s}, \underline{s}^{(\alpha)}}(i) - \bar{q}), \quad (1)$$

where $\int_{\underline{s}}$ denotes integration over configurations satisfying the local spherical constraint. For technical reasons it is preferable to take $\bar{q} < 1$: \underline{s} is only required to be close to $\underline{s}^{(\alpha)}$ outside $B_0(\ell)$. The results are qualitatively independent of \bar{q} if this is large enough. Next we define the correlation function

$$G(\ell) \equiv \mathbb{E} \{ \mathbb{E}_{\underline{s}^{(\alpha)}} [\langle Q_{\underline{s}, \underline{s}^{(\alpha)}}(0) \rangle_\ell^\alpha] \}, \quad (2)$$

where $\mathbb{E}_{\underline{s}^{(\alpha)}}$ and \mathbb{E} denote (respectively) averages over the reference configuration and the quenched disorder. The static length scale ℓ_s is the smallest ℓ such that $G(\ell) \leq \varepsilon$.

The averages $\mathbb{E}_{\underline{s}^{(\alpha)}}$ and \mathbb{E} can be taken by introducing replicas along the lines of [11]. Integrals over the spin variables are then traded for and $nr \times nr$ matrix order parameter $q_{ab}(i)$. Next we rescale the position to define $x = \gamma i \in [-\hat{L}, \hat{L}]^d$, $\hat{L} \equiv \gamma L$, and write (with an abuse of notation) $q_{ab} = q_{ab}(x)$, to get

$$G(\ell) = \lim_{\substack{n \rightarrow 0 \\ r \rightarrow 1}} \int q_{1,n+1}(0) e^{-\frac{1}{\gamma^d} S[q_{ab}]} d[q_{ab}]. \quad (3)$$

The dependency upon γ is now completely explicit and the functional integral can be performed using the saddle point method. Inspired by the solution of the mean field model [15], we look for a one-step replica symmetry breaking (1RSB) saddle point $q_{ab}^{\text{1RSB}}(x)$. This is characterized by three scalar functions $p(x)$, $q_1(x)$ and $q_0(x)$ and by a single Parisi 1RSB parameter m . While $p(x)$ is the local overlap between the reference configuration $\underline{s}^{(\alpha)}$ and the constrained one \underline{s} , $q_1(x)$ and

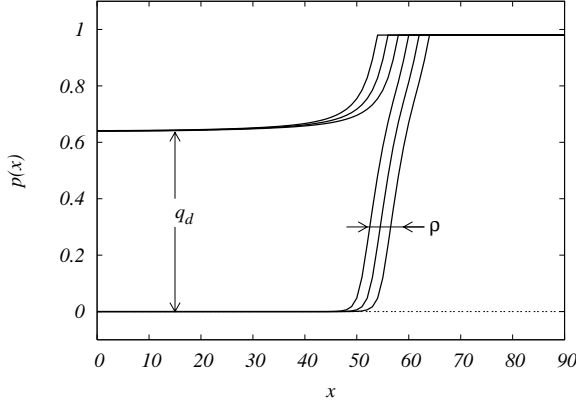


FIG. 2: Saddle points of the 1RSB action, cf. Eq. (4) for $T = 0.81365$ and several values of the ball radius $\hat{\ell}$. Here we plot the outcome of the iterative solution initiated with the $p(x) = \bar{q}$ identically. For $\hat{\ell} < \hat{\ell}_d = 59$, this is the high-overlap solution. For $\hat{\ell} > \hat{\ell}_d$ no high-overlap solution exists: the remaining dependence upon $\hat{\ell}$ is essentially a shift.

$q_0(x)$ are the overlaps of two constrained configurations when they belong (respectively) to the same or to different metastable states. Using this ansatz, one obtains $S[Q_{ab}] = n \int \mathcal{L}(x) d^d x + O(n^2)$, where

$$\begin{aligned} \mathcal{L} = & -\frac{\beta^2}{2} \{ f(1) + 2f(\psi * p) - (1-m)f(\psi * q_1) \\ & - mf(\psi * q_0) \} + \frac{1}{2} \frac{p^2 - q_0}{1 - (1-m)q_1 - mq_0} \\ & - \frac{m-1}{2m} \log(1 - q_1) - \frac{1}{2m} \log[1 - (1-m)q_1 - mq_0], \end{aligned} \quad (4)$$

with the various fields being evaluated at position x . Here we used the shorthand $\psi * q(x) = \int \psi(|x-y|) q(y) d^d y$. The constraint enforcing \underline{s} to be close to $\underline{s}^{(\alpha)}$ outside $B_0(\ell)$ is fulfilled by setting $p(x) = \bar{q}$ for $x \notin B_0(\hat{\ell})$ (notice the rescaling of the radius: $\hat{\ell} = \gamma \ell$).

Using Eq. (3), we obtain $\lim_{\gamma \rightarrow 0} G(\hat{\ell}/\gamma) = p(0)$, where $p(x)$ is evaluated at the minimum of the action $S_0 = \int \mathcal{L}(x) d^d x$. This implies that, as anticipated, $\hat{\ell}_s(T) = \gamma \ell_s(T, \gamma)$ has a finite $\gamma \rightarrow 0$ limit. We minimize the action looking spherically symmetric saddle points and iterating numerically the Euler-Lagrange equations for (4) until a stationary point is reached. We then repeat for several initial values of $p(x)$, $q_0(x)$ and $q_1(x)$ conditions, and compare the corresponding stationary points.

Since this procedure is relatively heavy from a computational point of view, we simplify the Lagrangian (4) in two ways. First, we expand the terms of the form $f(\psi * q)(x)$ in gradients of $q(x)$, and truncate to second order, thus obtaining $f(q) + cf'(q)\Delta q(x)$, where $c = \frac{1}{2d} \int z^2 \psi(|z|) d^d z$ (in our running example $c = 1$). Second, we discretize the model on a lattice of spacing h in the radial coordinate. Neither of these simplifications is expected to modify the qualitative behavior of

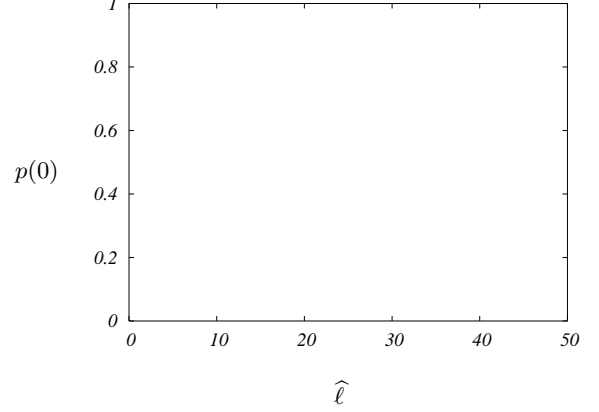


FIG. 3: Plot of the overlap $p(0)$ as a function of $\hat{\ell}$ in the approximated model with for $T = 1.0101, 0.9065, 0.8319, 0.8222, 0.81510, 0.8142 > T_d$ and $T = 0.7990 < T_d$. Inset: comparison between the approximate (analytical) and complete (numerical) minimization of the action for $T = 0.8222$.

the model, and we checked our predictions against alternative discretizations.

In Fig. 2 we show some typical results for $T \gtrsim T_d$. For small $\hat{\ell}$, a unique solution is found. The overlap $p(x)$ between the probe replica and the reference one is everywhere large: close to \bar{q} on the border, it saturates well inside the ball to a smaller value q_d roughly independent of the ball radius. The two overlaps $q_0(x)$, $q_1(x)$ are equal and close to $p(x)$. As $\hat{\ell}$ crosses some small value $\hat{\ell}_0$, a new solution appears, with $p(x)$ rapidly decaying to 0 in the interior of the ball, and the influence of the boundaries remaining confined to a small distance ρ . This solution describes a constrained replica \underline{s} well decorrelated from the reference one $\underline{s}^{(\alpha)}$, but has initially higher value of the free energy and is therefore thermodynamically irrelevant. The static length $\hat{\ell}_s$ is the smallest value of $\hat{\ell}$, such that the free energy of the low-overlap solution becomes smaller than the free energy of the high-overlap one. Above this length, the correlation between \underline{s} and $\underline{s}^{(\alpha)}$ in the center of the ball is small. However, the high-overlap solution persists as a metastable state. If the system is let evolve from the initial condition $\underline{s}^{(\alpha)}$ (and is constrained outside the ball), it will take an exponential (in $1/\gamma$) time to equilibrate. The high-overlap solution disappears at a larger radius $\hat{\ell}_d$. For $\hat{\ell} > \hat{\ell}_d$, the system is no more trapped in a metastable state selected by the reference configuration.

The evolution of different solutions as a function of $\hat{\ell}$ can be followed on Fig. 3, where we plot the overlap $p(0)$ between $\underline{s}^{(\alpha)}$ and \underline{s} at the center of the ball. For $T \gg T_d$, $p(0)$ is a single valued function of $\hat{\ell}$. Closer to T_d , multiple branches develop, with the coexistence region diverging as $T \downarrow T_d$. Beyond the high- and low-overlap solutions described above, an intermediate unstable branch is also present. In order to recover the full

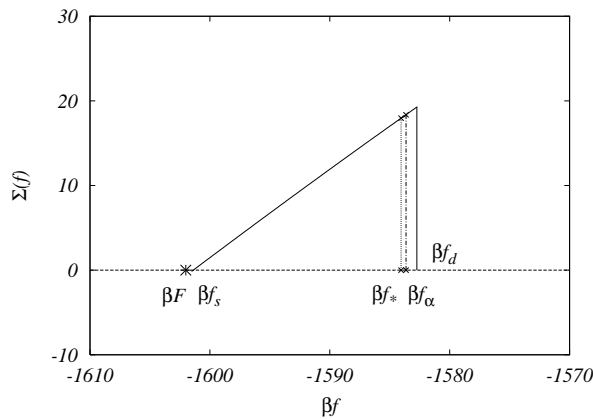


FIG. 4: Typical shape of the configurational entropy $\Sigma_{\hat{\ell}}(f)$ for $\hat{\ell}_s < \hat{\ell} < \hat{\ell}_d$ (here $T = 0.814 > T_d$, $\hat{\ell}_s \approx 16$, $\hat{\ell}_d \approx 41$, and $\hat{\ell} = 25$). Inset: configurational entropy $\Sigma_{\hat{\ell}}(f_*)/\hat{\ell}^d$ of the dominating metastable states as a function of $\hat{\ell}$. The curve crosses the axis at $\hat{\ell}^{1\text{RSB}}$ and ends at $\hat{\ell}_d$.

curve (including the unstable branch) we resorted to a simple approximation: we minimized the action under the constraint $p(x) = q_0(x) = q_1(x)$. In this setting, and under the “thin wall approximation” [16], the problem is equivalent to a one-dimensional mechanical system, and can be solved by quadratures. As shown in the inset of Fig. 3, the approximate and complete actions give results in good agreement. In particular, both cases yield the critical behaviors $\ell_s \sim (T - T_s)^{-1}$ and $\ell_d \sim (T - T_s)^{-1/4}$. Below T_d all three branches extend to infinity, indicating that activation is necessary on all length scales.

The complete 1RSB lagrangian (4) allows for a more precise description of the system. Consider T close to T_d and $\hat{\ell} \in [\hat{\ell}_0, \hat{\ell}_d]$ where $\hat{\ell}_0$ is the minimal length for multiple solutions. As anticipated, on the low overlap solution, we find $q_1 > q_0$. The interpretation is, as usual, that this solution does not describe a liquid phase, but rather a glassy one, with many pure states. The internal overlap of each such state is q_1 and the overlap between distinct states q_0 . The number of metastable states is exponential in $\ell = \hat{\ell}/\gamma$ for $\hat{\ell} > \hat{\ell}^{1\text{RSB}}$ (the action is maximized by $m = 1$) and subexponential for $\hat{\ell} < \hat{\ell}^{1\text{RSB}}$ ($m < 1$). RSB slightly modify the free energy of the low overlap solution for $\hat{\ell} < \hat{\ell}^{1\text{RSB}}$ thus changing the value of ℓ_s .

Let us reconsider the thought experiment of letting the system evolve starting from the reference configuration $\underline{s}^{(\alpha)}$. The system escapes the metastable state selected by $\underline{s}^{(\alpha)}$ in a time exponential in $1/\gamma$. After that, however, it does not equilibrate freely within the rest of phase space, but rather moves through activation from one state to the other, spending an exponential time in each one.

By taking the Legendre transform of the m -dependent free energy, we can compute the configurational entropy $\Sigma_{\hat{\ell}}(f)$ (i.e. the log number of metastable states as a function of their *internal* free-energy f) [?]. In Fig. 4 we

show an example of its behavior for $\hat{\ell}_s < \hat{\ell} < \hat{\ell}_d$. An exponential number of metastable states is present in an $\hat{\ell}$ -dependent free energy interval $[f_1, f_2]$ (most of them having free energy f_2). The dominating ones have free energy f_* determined by maximizing $\Sigma_{\hat{\ell}}(f) - \beta f$. The free energy F_+ of the high overlap state is lower than for most of other metastable states $F_+ < f_2$ (because of the better matching with the boundaries) but higher than the overall free energy $F_- = f_* - T\Sigma_{\hat{\ell}}(f_*)$. If $\hat{\ell}$ is decreased, the gap between F_- and F_+ decreases. At $\hat{\ell}^{1\text{RSB}}$ the configurational entropy $\Sigma_{\hat{\ell}}(f_*)$ vanishes and $F_- = f_* = f_1$. Eventually F_- and F_+ cross at $\hat{\ell} = \hat{\ell}_s < \hat{\ell}^{1\text{RSB}}$. If on the other hand $\hat{\ell}$ is increased, the configurational entropy increases as well, until the 1RSB solution ceases to exist. This happens at the dynamical length $\hat{\ell}_d$, coherently with the fact that beyond this scale relaxation does not require activation.

For a small non-vanishing γ , the above picture should remain roughly correct. However, activated and MCT time scales must now be compared. The first one corresponds a typical relaxation time $\tau_{\text{act}} \sim \exp\{\Upsilon\ell_s^\psi\}$, while the second gives $\tau_{\text{MCT}} \sim \ell_d^z$. Therefore, MCT behavior is faster and dominates until very close to T_d . The divergence is then cut-off when $\ell_d(T) \approx \exp\{\Upsilon\ell_s(T_d)^\psi/z\}$, and dynamics becomes activated at lower temperatures. During this cross-over, the physical dynamical length ξ_d characterizing the size of cooperatively rearranging regions crosses over from $\xi_d \approx \ell_d$, to $\xi_d \approx \ell_s$.

Summarizing we implemented the mean-field theory of mosaic state in a microscopic model. This allowed to establish relations between mosaic and MCT dynamical lengths which had not been predicted from phenomenological considerations. The dynamical length scale is defined by the property that dynamics is dominated by activation at shorter scales. It can further be identified with the one appearing in the MCT divergence of four point susceptibilities. Below mosaic length the system is instead rigid for thermodynamic reasons. The two happen to be close above the MCT critical temperature and widely separated between this and the glass transition, corresponding to the crossover between relaxational and activated dynamics.

Acknowledgments We thank the participants of the programme “Principles of the Dynamics of Non-Equilibrium System” 9 January - 30 June 2006, Isaac Newton Institute, Cambridge and in particular D. Mukamel for important discussions. This work was supported in part by the EU under contract “HPRN-CT-2002-00319 STIPCO”.

- [1] S. Das, Rev. Mod. Phys. **76** (2004) 785
- [2] T. R. Kirkpatrick and P. G. Wolynes, Phys. Rev. B **36** (1987) 8552; T. R. Kirkpatrick, D. Thirumalai, and P. G. Wolynes, Phys. Rev. A **40** (1989) 1045

- [3] P. G. Wolynes, Jour. Res. NIST **102** (1997) 187, X. Xia, P. G. Wolynes, Proc. Nat. Acad. Sci. **97**, (2000) 2990, Phys. Rev. Lett **86** (2001) 5526
- [4] J.-P. Bouchaud and G. Biroli, J. Chem. Phys. **121** (2004) 7347
- [5] F. Ritort and P. Sollich, Adv. Phys., **52** (2003) 219 and references therein.
- [6] C. Donati, S. Franz, G. Parisi, and S. C. Glotzer, J. Non-Cryst. Solids **307-310** (2002) 215, S. Franz and G. Parisi J. Phys.: Condens. Matter bf 12 (2000) 6335
- [7] G. Biroli, J.-P. Bouchaud, Europhys. Lett. **67** (2004) 21
- [8] L. Berthier, G. Biroli, J.-P. Bouchaud, L. Cipelletti, D. E. Masri, D. L'Hte, F. Ladieu, and M. Pierno Science **310** (2005) 1797
- [9] R. L. Jack, J. P. Garrahan J. Chem. Phys. 123, 164508 (2005)
- [10] S. Franz and F. L. Toninelli Phys. Rev. Lett. **92** (2004) 030602, J. Phys. A: Math. Gen. **37** (2004) 7433, J. Stat. Mech. (2005) P01008
- [11] S. Franz, J. Stat. Mech. (2005) P04001, Europhys. Lett. **73** (2006) 492
- [12] A. Montanari and G. Semerjian, cond-mat/0509366
- [13] A. Montanari and G. Semerjian, cond-mat/0603018 emi
- [14] G. Biroli, J.-P. Bouchaud, K. Miyazaki and D. Reichman, cond-mat/0605733.
- [15] S. Franz and G. Parisi, J. Phys. I (France) **5** (1995) 1401, Phys. Rev. Lett. **79** (1997) 2486
- [16] J. S. Langer, Ann. Phys. **41** (1967) 108, **54** (1969) 258
- [17] R. Monasson, Phys. Rev. Lett. **75** (1995) 2847
- [18] M. Dzero, J. Schmalian, and P. Wolynes, Phys. Rev. B **72** (2005) 100201